Journal of the Korean Magnetic Resonance Society **2016**, *20*, 50-55
DOI 10.6564/JKMRS.2016.20.2.050

Backbone assignment of the anticodon binding domain of human Glycyl-tRNA synthetase

Ameeq Ul Mushtaq[1], Hye Young Cho[1] , Youngjoo Byun[1] and Young Ho Jeon[1]

[1]College of Pharmacy, Korea University, Sejong-ro 4211, Sejong 30019, South Korea

Received May 3, 2016; Revised May 27, 2016; Accepted June 3, 2016

Abstract Backbone ^{1}H, ^{13}C and ^{15}N resonance assignments are presented for the anticodon binding domain (residues 557-674) of human glycyl-tRNA synthetase (GRS). Role of the anticodon binding domain (ABD) of GRS as an anticancer ligand has recently been reported and its role in other diseases like Charcot–Marie–Tooth (CMT) and polymyositis have increased its interest. NMR assignments were completed using the isotope [$^{13}C/^{15}N$]-enriched protein and chemical shifts based secondary structure analysis with TALOS+ demonstrate similar secondary structure as reported in X-ray structure PDB 2ZT8, except some C-terminal residues. NMR signals from the N-terminal residues 557 to 571 and 590 to 614 showed very weak or no signals exhibiting dynamics or conformational exchange in NMR timescale.

Keywords Glycyl-tRNA synthetase, anticodon binding domain(ABD), backbone assignment

Introduction

Glycyl-tRNA synthetase (GRS) is an important component of the translation apparatus and recently reported proapoptotic activity of secreted GRS implicates its functions beyond translation.[1] Its causative role in Charcot–Marie–Tooth (CMT) disease and polymyosits makes GRS of increasing interest.[3] It is reported that GRS is an anticancer protein ligand which is abundant in serum and is secreted from macrophages in response to Fas ligand, it binds with cadherin (CDH)6 and releases phosphatase 2A (PP2A) from (CDH)6 in ERK-activated tumor cells. The activated PP2A then suppresses ERK signaling through dephosphorylation of ERK and induces apoptosis.[1,2] Role of GRS anticodon binding domain have been demonstrated in above mentioned reports. We designed the GRS-ABD (557-674 and 538-674) constructs and perform NMR study. Here we report the backbone assignment of GRS-ABD (557-674).

Experimental Methods

Sample preparation- Glycyl-tRNA synthetase ABD(557-674, 538-674) plasmids was gifted from Seoul National University. After optimizing expression and purification conditions in LB medium, the transformed *E.coli* BL21(DE3) cells(Novagen) were grown in M9 minimal medium at 37 ºC. Isotope-enriched glycyl-tRNA synthetase ABD proteins ([^{15}N] and [$^{13}C/^{15}N$]) were prepared for NMR studies in M9 medium that were supplemented

* Address correspondence to: **Young Ho Jeon,** College of Pharmacy, Korea University, Sejong-ro 4211, Sejong 30 019, South Korea, Tel: 82-41-860-1615; Fax: 82-41-860-1606; E-mail: yhjeon@korea.ac.kr

with [^{13}C]glucose and/or [^{15}N]NH4Cl (^{13}C: D-Glucose (U-$^{13}C_6$, 99%), ^{15}N: Ammonium Chloride (^{15}N, 99%), Cambridge Isotope Laboratories) as the sole source of carbon and nitrogen. When the O.D600 of cell growth reached about 0.6, protein expression was induced by adding IPTG (Duchefa) at a final concentration of 0.5 mM, and the induction was prolonged for 3h. The harvested cells were then disrupted by sonication, and from the supernatant the glycyl-tRNA synthetase ABD proteins was purified via sequential chromatography on a GST column (GSTrapTM HP, GE Healthcare) and a gel-filtration column (Hiload 16/60 SuperdexTM 200 Prep Grade, GE Healthcare). The fused GST tag was cleaved with the protease thrombin, followed by the removal of GST and other impurities via the application of gel-permeation chromatography. Finally, the purified solution was concentrated and buffer-exchanged by ultrafiltration (Amicon). Protein concentration was estimated via typical Bradford and BCA assays.

NMR Studies- NMR spectra were recorded on Avance 600-MHz NMR spectrometer equipped with a triple-resonance probe (Bruker, Germany), with uniformly [^{13}C/^{15}N] labeled 0.3mM GRS-ABD protein sample in 20mM HEPES (pH 6.5), 80 mM NaCl, 1mM PMSF, 1mM EDTA, 1mM DTT and 10% D2O at 308K. Number of signals in ^{1}H-^{15}N HSQC were better at 308K, under the optimized condition data for triple resonance experiments HNCA, HN(CO)CA , HNCACB, CBCA(CO)NH, HNCO, HN(CA)CO, HBHANH and HBHA(CO)NH were acquired.

NMR spectra were processed using NMRPipe and NMRDraw software[4] (Delaglio et al. 1995) and visualized as well as analyzed using CCPN2.1.5 (Wim F. Vranken et. al.).[5] Sequential backbone NMR assignments for ^{15}N, ^{13}Cα, ^{13}Cβ, ^{13}C', ^{1}Hβ,, ^{1}Hα and ^{1}HN atoms were performed by verifying and linking of resonances, according to the inter- residue ^{13}C, ^{1}H correlations. Assigned chemical shifts were directly referenced to DSS for the ^{1}H while ^{13}C and ^{15}N atoms were referenced indirectly as suggested in BMRB(://www.bmrb.wisc.edu). Secondary structure prediction was done with TALOS+, a public domain software's that predicts secondary structure from ^{1}HN,

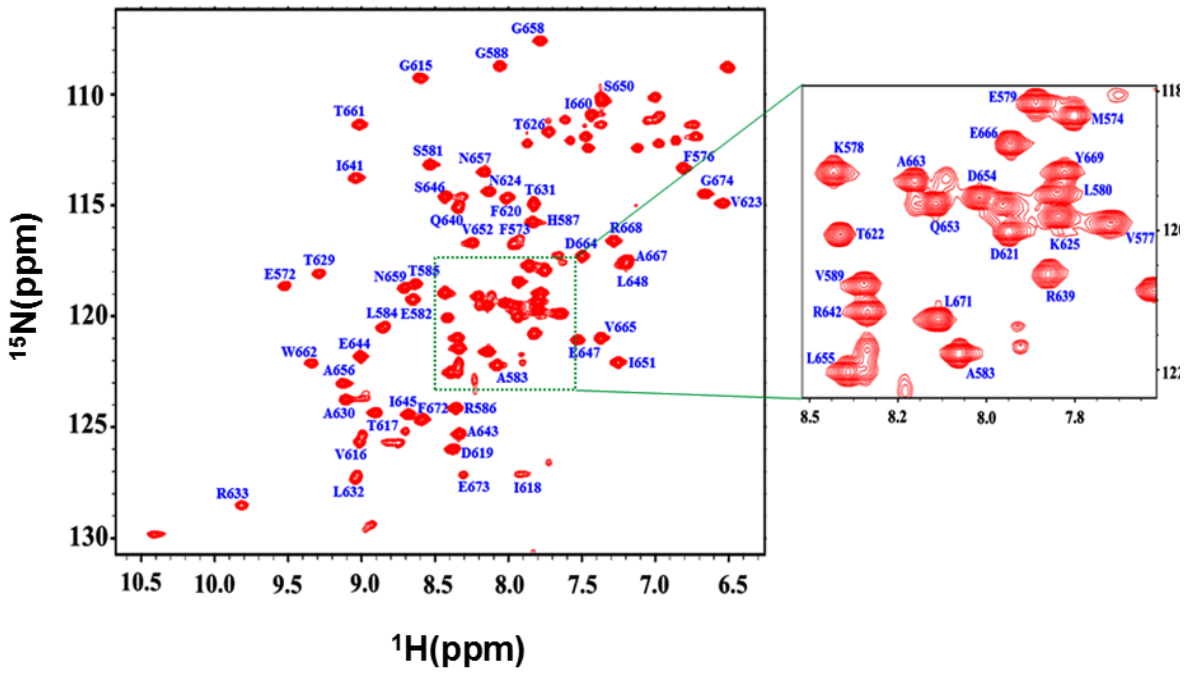

Figure 1. 2D [^{1}H/^{15}N] HSQC spectrum showing backbone assignment of GRS-ABD (557-674) at 308K.

^{15}N, $^{13}C\alpha$, $^{13}C\beta$, $^{13}C'$ chemical shift data using similarity approach.[6]

Results and Discussion

Backbone $^{13}C_{\alpha}$, $^{13}C_{\beta}$, $^{13}C'$, ^{15}N and $^{1}H_{N}$ resonances were unambiguously assigned for 73 residues of GRS-ABD (557-674), based on intra- and sequential correlations in 3D spectra. In ^{1}H-^{15}N HSQC spectrum, we could observe 86 out of expected 111 peaks. 85% of the backbone resonances were assigned. The amide signals from N-terminal 557-571 and 590-614 residues are absent or very weak in spectra possibly due to dynamics or conformational exchange of the protein in NMR time scale. Similar phenomenon was observed with GRS-ABD (538-674) construct. Table 1 summarizes the sequence-specific backbone NMR assignments of the construct GRS-ABD (557-674). TALOS+ prediction showed similar secondary structure profiles as in the X-ray structure PDB 2ZT8, except C-terminal residues from 671-673 which show propensity to beta conformation in solution state. T1ρ/T2 profile of GRS-ABD along residue number identified the residues with conformational exchange, starting and ending residues in 557-571 and 590-614 fragments exhibit higher values of $T_{1\rho}/T_2$ indicating dynamics of these fragments in micro to milliseconds NMR time scale (data not shown).

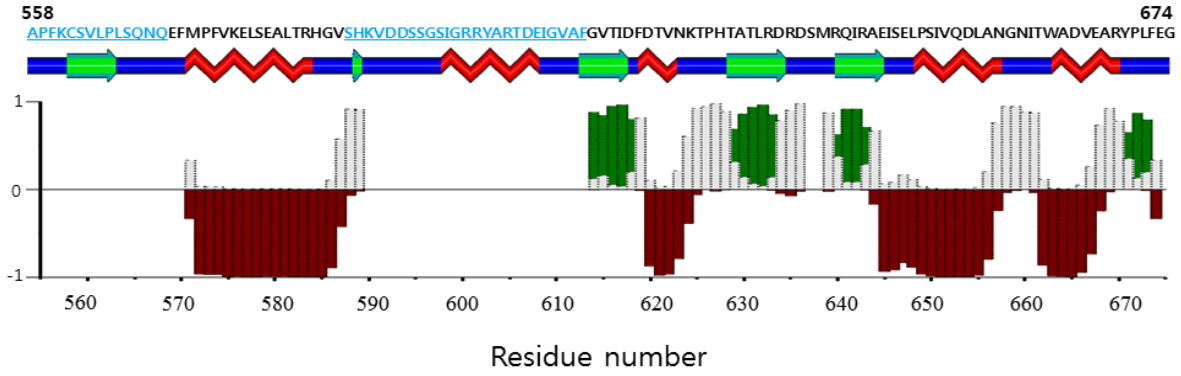

Figure 2. Comparison of secondary structure of GRS-ABD from X-ray structure PDB 2ZT8 with TALOS+ based secondary structure from assigned chemical shift data of GRS-ABD(557-674). Maroon bars show alpha helical, green and grey bars show beta and coil propensities respectively. Regions 557-571 and 590-614 in sequence are colored in light blue.

Table 1. Chemical shift table of Glycyl-tRNA synthetase ABD(557-674) at 308K.

Residue	^{1}HN	^{15}N	$^{13}C^{\alpha}$	$^{13}C^{\beta}$	^{13}CO	$^{1}H^{\alpha}$	$^{1}H^{\beta}$
E572	9.521	118.64	59.13	28.72	177.86	4.236	2.114
F573	7.960	116.72	59.70	40.25	178.41	4.369	3.301, 2.862
M574	7.753	117.94	59.08	29.42	175.35	4.527	2.365, 2.170
P575	-	-	66.36	31.22	179.00	4.185	2.134, 1.176
F576	6.809	113.31	61.22	39.37	177.68	4.052	3.026 , 2.813
V577	7.647	119.86	66.94	32.17	177.14	3.300	2.362
K578	8.432	118.94	59.80	32.67	178.51	3.986	1.833

E579	7.860	117.70	59.49	29.36	179.35	4.022	2.044, 1.933
L580	7.999	119.31	57.76	41.47	178.02	4.207	1.735, 1.640
S581	8.533	113.16	60.74	63.31	-	-	-
E582	8.648	119.24	59.93	29.10	179.55	4.050	2.047, 2.173
A583	8.078	122.21	55.40	19.29	180.88	4.185	1.612
L584	8.846	120.50	59.13	40.54	179.44	3.862	1.427
T585	8.632	118.54	67.38	68.41	-	4.114	4.483
R586	8.355	124.13	59.85	30.10	177.91	4.106	2.050, 1.924
H587	7.832	115.77	57.22	29.60	174.52	4.438	3.404
G588	8.057	108.72	46.63	-	174.74	4.014	-
V589	8.346	120.96	61.72	32.31	175.55	4.108	2.043
V593	8.739	125.70	61.91	31.95	175.39	-	-
D594	8.929	129.38	54.16	-	-	-	-
G615	8.601	109.26	44.90	-	172.81	-	-
V616	9.013	125.66	60.16	34.50	175.30	5.485	-
T617	8.902	124.34	61.65	70.32	173.46	5.175	4.049
I618	7.912	127.11	60.13	-	173.64	-	-
D619	8.376	125.98	51.72	43.44	175.35	4.864	2.489
F620	8.012	114.67	62.74	38.38	178.23	4.128	3.190
D621	7.937	120.02	57.54	39.96	179.56	4.492	2.549
T622	8.412	120.07	66.40	68.40	174.62	4.301	4.175
V623	6.539	114.90	64.23	32.68	177.43	3.050	1.735
N624	8.129	114.37	55.12	40.35	175.52	4.681	2.800
K625	7.795	119.74	55.38	34.44	173.36	4.616	1.768
T626	7.722	111.67	58.30	70.72	173.75	3.862	3.736
T629	9.288	118.08	59.31	72.31	172.41	5.048	3.806
A630	9.107	123.76	50.32	22.40	174.41	4.487	1.207
T631	7.826	114.94	61.39	70.24	172.99	4.988	-
L632	9.041	127.30	53.19	44.86	173.53	5.364	-
R633	9.817	128.52	54.02	33.21	175.00	5.111	-
R639	7.826	120.78	57.14	32.21	174.75	4.365	
Q640	8.341	115.10	54.55	34.25	175.89	6.152	2.111
I641	9.037	113.75	58.54	43.26	174.71	5.238	1.865
R642	8.336	121.45	54.63	33.32	174.50	4.987	1.862

A643	8.331	125.30	50.28	22.63	175.84	4.688	0.680
E644	9.007	121.82	58.60	29.63	178.44	4.181	2.298, 1.985
I645	8.680	124.42	65.42	38.66	176.81	3.799	1.763
S646	8.428	114.61	60.42	62.81	-	4.238	3.999
E647	7.526	121.06	56.73	31.01	177.14	4.425	2.055
L648	7.201	117.65	59.11	40.95	174.31	3.913	1.466
P649	-	-	67.14	30.34	176.68	3.742	1.505
S650	7.361	110.31	61.42	62.82	-	-	3.864
I651	7.251	122.07	64.98	38.65	177.79	3.676	1.613
V652	8.244	116.69	67.03	30.88	177.10	3.115	1.798
Q653	8.143	119.51	59.76	28.72	177.59	3.856	2.240, 1.990
D654	8.020	119.40	57.65	40.14	179.77	4.678	2.823, 2.449
L655	8.391	122.53	57.40	42.74	181.19	4.178	1.550, 1.237
A656	9.128	123.03	55.13	17.96	179.25	4.236	1.550
N657	8.163	113.50	53.05	38.85	176.04	4.863	2.987
G658	7.782	107.58	46.10	-	174.55	4.179	4.030
N659	8.707	118.73	55.17	39.10	175.50	4.613	2.865, 2.671
I660	7.434	110.90	59.06	41.64	174.00	4.735	2.175
T661	9.014	111.35	59.87	72.72	175.94	4.802	-
W662	7.337	122.12	60.71	29.00	177.25	4.175	3.487, 3.187
A663	8.202	119.10	55.36	18.23	180.93	4.022	1.417
D664	7.496	117.27	57.39	40.94	178.57	4.303	3.113, 2.611
V665	7.370	120.97	66.72	30.70	178.18	3.462	1.626
E666	7.933	118.44	59.04	29.47	177.47	3.864	1.953, 1.798
A667	7.188	117.47	53.40	18.53	178.67	4.237	1.474
R668	7.282	116.59	56.87	33.34	175.15	4.112	1.486
Y669	7.779	118.95	56.13	40.14	172.32	4.925	3.179, 2.394
P670	-	-	62.59	32.30	176.78	4.490	2.311, 2.008
L671	8.136	121.59	55.48	42.88	177.47	4.672	1.678
F672	8.588	124.66	57.20	41.64	174.54	4.855	2.862, 2.717
E673	8.306	127.16	56.13	30.65	174.77	4.273	1.990, 1.739
G674	6.660	114.48	46.17	-	178.42	-	3.551

Acknowledgements

This study was supported by a grant NRF-2013M3A6A4045160 and NRF-2014R1A4A1007304 funded by Ministry of Science, ICP and Future Planning (MISP) of Korea. We thank to Dr. Eunha Hwang and Mrs. Eun-Hee Kim for their support for NMR measurements in Korea Basic Science Institute.

References

1. M. C. Park, T. Kang, D. Jin, J. M. Han, S. B. Kim, Y. J. Park, K. Cho, Y. W. Park, M. Guo, W. He, X. L.Yang, P. Schimmel, and S. Kim, *Proc. Natl. Acad. Sci. U S A* **109**, E640 (2012)
2. N. R. Gough, *Sci. Signal*. **5**, ec83 (2012)
3. W. William Motley, K. Talbot, Kennerh, and H. Fischbeck, *Trends in Neurosciences* **33**, 59 (2010)
4. F. Delaglio, S. Grzesiek et al. *J. Biomol. NMR* **6**, 277 (1995)
5. W. F. Vranken, W. Boucher, T. J. Stevens, R. H. Fogh, A. Pajon, M. Llinas, E. L. Ulrich, J. L. Markley, J. Ionides, and E. D. Laue, *Proteins* **59**, 687 (2005)
6. Y. Shen, F. Delaglio, G. Cornilescu, and A. Bax, *J. Biomol. NMR* **44**, 213 (2009)
7. T. K. Hitchens and G.. S. Rule, *Fundamentals of protein NMR spectroscopy* Berlin, Springer (2005)